Theor Chem Acc (2012) 131:1195
DOI 10.1007/s00214-012-1195-x

REGULAR ARTICLE

The first solvation shell of Reichardt's dye in ionic liquids: a semiempirical study

Cinzia Chiappe · Christian Silvio Pomelli

Received: 15 July 2011 / Accepted: 16 February 2012 / Published online: 2 March 2012
© Springer-Verlag 2012

Abstract The nature of solvation of Reichardt's dye in ionic liquids is investigated through semiempirical calculations. We build on the basis of electrostatic considerations a cluster of three ionic pairs that represent the first solvation shell of the dye. The spatial organization of this shell is a balance between sterical, electrostatic and, in the case of functionalized ionic liquids, specific interactions. This model is not sufficient to obtain values of ET(30) quantitatively comparable to the experimental ones, but some qualitative features can be rationalized. The resulting scenario of solute–solvent interactions is different with respect to molecular solvents. Thus, we suggest caution in comparing ionic and molecular solvents through solvatochromic scales.

Keywords Ionic liquids · Solvatochromic probes · PM6 · ZINDO · Reichardt's dye · CIS

1 Introduction

Recent years have seen a growing experimental focus on a novel class of solvents known as room-temperature ionic liquids (ILs). Generally constituted by an organic cation and a polyatomic anion, these salts liquid at or near room temperature have been found capable of solvating a wide range of organic, inorganic and polymeric compounds. The dissolution ability, however, strongly depends on cation and anion structure and the nature of the solute–solvent interactions responsible for their solvation properties remain one of the central themes in the ionic liquid research [1, 2]. Normally, the most important quantity determining the choice of a solvent is its polarity. In molecular liquids, polarity may be qualitatively understood by examination of the electrostatic dipole moment and hydrogen-bonding properties of individual solvent molecules. On the basis of these elements, it is possible to predict the solubility of a substrate in a selected solvent and the effects of the solvent on some reaction parameters, such as reaction rate. But, by definition, ions carry a nonzero electrostatic monopole moment (charge) that should dominate dipolar and higher-order terms. Furthermore, cation–anion interactions lead to considerable charge ordering in ILs, producing in particular in ILs bearing sufficiently long alkyl chains on cation or anion, an inhomogeneous environment characterized by polar and not polar regions. The unique nature of this environment makes often the application of models and concepts developed for molecular solvents suspect or misleading. Understanding polarity of ILs and their solvent power, therefore, may require a careful rethinking of the fundamental nature of solvation.

An experimental approach to evaluate such interactions and define polarity is the examination of the behavior of a chromophore in the medium of interest. Spectrophotometric studies of chromophores have been carried out both in molecular solvents and ILs showing that the solvatochromic properties of these latter media depend on the structure of cation and anion and their combination [3–8]. The effects due to a specific cation

Dedicated to Professor Vincenzo Barone and published as part of the special collection of articles celebrating his 60th birthday.

Electronic supplementary material The online version of this article (doi:10.1007/s00214-012-1195-x) contains supplementary material, which is available to authorized users.

C. Chiappe · C. S. Pomelli (✉)
Dipartimento di Chimica e Chimica Industriale,
Via Risorgimento 35, 56126 Pisa, Italy
e-mail: cris@dcci.unipi.it

are significantly affected by the counterion. Creating cation–anion interactions that compete with specific cation–solute or anion–solute interactions can control the polarity of the resulting IL.

To date, there have been relatively few simulation studies of IL systems, and most of these have centered on the structural, transport and thermodynamic properties of ILs. However, in 2004, a molecular dynamics simulation study was carried out to investigate the nature of solvent polarity in an IL system calculating the absorption spectrum of the Reichardt's dye 30 in 1-butyl-3-methylimidazolium hexafluorophosphate, [bmim][PF_6], and determining the solute–solvent interactions responsible for the solvatochromic shift [9]. This spectroscopic shift is a well-known indicator for polarity that has been widely applied to define IL polarity.

Here, we report a computational study using semiempirical methods to characterize the first solvation shell of some ILs. In a recent paper [10], we have reported a large set (about 60) of measures of ET(30) [11] and Kamlet Taft solvatochromic parameters [12] for different kinds of ILs. From this study emerges that:

1. as expected, ET(30) and α values are linearly correlated;
2. the range in which π^* values spreads is very small;
3. the values of β depend principally by the anion where ET(30) and α values depend on the cation;
4. the ET(30) and α values are strongly anion dependent. More coordinating anions, such as dicyanamide, are able to reduce the hydrogen bond ability of a specific cation.

Therefore, we decided to study computationally a subset of ILs that contain this anion and cations where the charge is carried out by a quaternary nitrogen enclosed in an aliphatic heterocyclic ring, for which experimental measurements suggested the presence of peculiar structural effects. Since the alkyl chain length on nitrogen and the heterocyclic ring size appeared to affect significantly the ET(30) and α values, we have included in this computation study different kind of rings and sidechains. Moreover, some sidechains presents one or more alcoholic moieties; the presence of this group significantly increases IL polarity increasing ET(30) and α values. The dicyanamide ILs shows a very narrow range of β values; thus, ET(30) (or α) is the only index that can discriminate between these ILs. The interactions between the IL components and the Reichadts dye, which determine the ET(30) and α values, are, therefore, fundamental for the rationalization of the solvation ability of these ILs.

Results arising from this investigation show that the solvation shell of Reichardt dye in ILs is the result of interplay between chemical, sterical and electrostatic factors.

2 The method and the model system

The remarkable size of the Reichardt's dye 30 is a challenge to computational methods. If the system do not consist of the dye only but include also some solvent molecules, the computational costs become prohibitive. Also, a RISM-KH description of ILs [13] is too computationally expensive. The MD-based study of Kobrak and Znamenskiy [9] give a nice picture of these kinds of systems both at local and global level. We refer to some results of this study when discuss our results. The use of semiempirical methods to study specific and bulk effect of solvent on Reichardt's dye is reported in a paper by Caricato et al. [14]. In this paper, the geometry of ET(30)-solvent clusters has been optimized using AM1 [15] semiempirical method followed by a ZINDO [16] calculation of the excited state. The aim of this paper is to describe specific effect of the solvent ions on the ET(30) solute, and thus, we prefer the semiempirical protocol rather than the MD one.

We decided to use the PM6 method, introduced by Steward in 2007 [17] and documented by the same author in a series of applicative papers [18, 19]. PM6 is one of the most recent semiempirical parameterizations of general use and in fact replace AM1 and PM3 [20]. PM6 is parameterized for a large number of chemical elements. This can be useful for future extensions to a larger set of ILs. We considered also DFTB [21] in its DFTB+ [22] implementation, but this method, at the present, is parameterized for fundamental organic elements and few metals. Furthermore, DFTB+ package does not allow performing excited states calculations. PM6 has been well received in the computational chemistry community (more than 200 papers reporting PM6 results in 2010 only). For this study, we used the implementation of PM6 in the Gaussian 09 package [23]. This implementation provides an interface with the CIS method for excited states [24]. We use both CIS/PM6 and ZINDO at PM6 geometries for the calculation of ET(30). We try also to perform some TDDFT calculations on the PM6 optimized geometries, but the hardware and CPU time requirement are beyond our computational resources. Finally, we considered also the use of IEFPCM [25] to estimate the bulk effect, but the values of dielectric constants of ILs are still a debated question [26, 27]. Some test calculations with an arbitrary dielectric constant of 20 lead to very chaotic behaviors, significantly worse than those in vacuo. Thus, we decided to avoid performing exhaustive IEFPCM calculations.

We adopt the supermolecular approach that has been already used to describe ILs features as reactivity [28, 29], solubility of small molecules [30] and ionic pairing [31]. The construction of the first shell is limited to the zones of the space that are immediately adjacent to the N and O

atoms of the dye. For reasons of simplicity, we assume that they lie on the horizontal plane with an upper and lower side. The spatial arrangement of phenyl groups around the N atom leads to two narrow and equivalent holes one on the upper and the other on the lower side of the dye. The spatial accessibility of this moiety is limited. Since the N atom carries a positive charge, we place one anion (in this context dicyanamide only) near each of the holes. Two cations are placed nearby the oxygen atom. Another anion is inserted between the two cations. A third cation is inserted, to reach the electroneutrality near the third anion. This arrangement, which presents a strictly alternating of positive and negative centers, is schematized in Fig. 1.

When we tried to optimize the geometries using the standard Berny [32] algorithm of Gaussian 09, we had some troubles. This may be attributed to the fact that the system is very complex: there are seven not bounded groups of atoms and thus 36 intermolecular degrees of freedom. In fact, a consistent number of Berny optimizations did not converge showing a chaotic behavior. This is typical of complex system that reaches an energy plateau in the phase space. We decided to fix this issue by restarting from the point with the smallest gradient RMS using the GDIIS [33] algorithm. After this treatment, the structure converged in few steps. This does not introduce artifacts in the final obtained geometry since the structure acceptance criterion is the same. All the structures have been characterized as local minimums by frequency calculations. However, in these complex systems, there is not an absolute certain to have reached the global minimum. The final structures obtained for the different systems studied show, looking to geometrical parameters and by visual inspection, a degree of similarity and reasonability sufficient to ensure to have obtained, at least, snapshots representative of the real systems. On the optimized structures have been performed CIS/PM6 and ZINDO calculations of excited states. The number of states being optimized is 10.

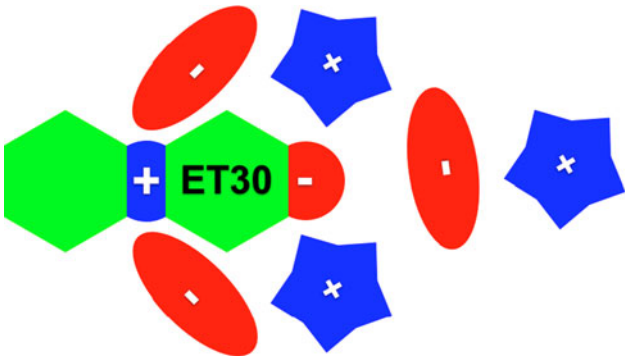

Fig. 1 Schematic representation of the first solvation shell of Reichardt's dye in a ionic liquid. The phenyl wings surround the zwitterionic part of the dye. The positive center (nitrogen, in *blue*) is sterically hindered. Nearby the nitrogen we found two anions on the *top* and *bottom* side. Two cations coordinate the oxygen. A further ionic pair is introduced in this region: the anion shields the two coordinating cations, and the cation determines the electroneutrality

3 Results and discussion

The results are arranged in Tables 1 and 2. In Table 1 are reported some geometrical quantities that define the geometry of the ionic clusters here considered. In Table 2 are reported the ET(30) values and the variation of HOMO and LUMO energies with respect the isolated dye. Some explicative molecular graphics are reported in Figs. 2, 3 and 4.

First, we analyze the geometrical quantities reported in Table 1. In particular, we start analyzing IL cation–dye interactions.

In this investigation, we have considered four aliphatic cations (pyrrolidinium, piperidinium, morpholinium and azepanium) characterized by localized quaternary nitrogen charged center (Scheme 1) and bearing a methyl group and an alkyl chain on nitrogen or a methyl group and a hydroxylethyl or a glyceryl group associated with the dicyanamide anion. In these systems, the center of the positive charge cannot interact directly with the dye oxygen; the interaction occurs through some hydrogen atoms. In Table 1, we report all the hydrogen atoms of cations that are <2.5 Å apart from the dye oxygen. Depending on cation structure, these hydrogens can be those of the ring in α positions with respect to the charged nitrogen (labeled as R), on the aliphatic chains (labeled by the number corresponding to the chain length 1, 2, 4, 8 and with the position α, β) or on the alcoholic moiety (OH) for 1,e and 1,g cations (in this latter case, we label as "e" the OH group nearest to the ring. However, we did not observe coordination by the further OH).

If the cation is functionalized with one or two hydroxyl groups on the alkyl chain, only the OH group closer to the ring is coordinated to the oxygen atom of Reichardt's dye. Furthermore, in this coordination is also involved one the four hydrogens of the ring located in the α positions. The coordination of the two cations is very similar. In the case of N-methyl-N-glycerylpiperidinium, $Pip_{1,g}$, reported in Fig. 2, there is no direct interaction between the terminal OH group and the dye oxygen. Probably, a chelation of the dye oxygen with two OH groups of the same cation takes away the second cation weakening the electrostatic interaction of this last one with the dye positive center. In this case, the electrostatic interaction appears to prevail on chelating effect. The terminal OH is thus free to coordinate other cations.

The pattern of interactions of non-functionalized cations is more complex. In this case, there is a neat distinction

Table 1 Geometrical quantities

Cation	N-A1	N-A2	O-C1	O-C2
$Pyr_{1,2}$	3.093(T)	3.207(T)	1.999(1), 2.099(R), 2.375(2β)	2.018(R)
$Mor_{1,e}$	3.179(T)	3.220(T)	1.751(e), 2344(R)	1.774(e), 1.988(R)
$Mor_{1,2}$	3.097(T)	3.283(T)	1.884(R), 2.093(1), 2.102(2β)	1.987(R)
$Mor_{1,4}$	3.117(T)	3.282(T)	1.934(R), 2.101(1)	2.034(R)
$Mor_{1,8}$	3.094(T)	3.309(T)	1.905(R), 2.162(1), 2.287(8α)	2.020(R)
$Pip_{1,e}$	3.174(T)	3.175(T)	1.776(e), 2168(R)	1.723(e), 2.312(R)
$Pip_{1,g}$	3.149(T)	3.234(T)	1.704(e)	1.735(e), 1.987(R)
$Aze_{1,4}$	3.234(T)	3.296(T)	2.207(R), 2.239(4β)	2.596(R)
$Aze_{1,e}$	3.131(T)	3.155(T)	1.788(e), 2.245(R)	1.724(e), 2.469(R)

All the data are expressed in Å

N, O Reichardt's dye heteroatoms, *A1, A2* nearest and next nearest anion, *C1, C2* nearest and next nearest cation, *T* terminal coordination of the anion, *R* coordination at hydrogen on the ring, *1, 2, 8* coordination at hydrogen on the sidechain (with the relative position), *e* coordination with alcoholic hydrogen

Table 2 Experimental and theoretical results for ET(30) parameters for the ionic liquids here considered

Cation	ET(30) exp[a]	ET(30) ZINDO	ET(30) CIS/PM6	ΔHOMO	ΔLUMO
In vacuo	27.10	26.75	38.77	0.00	0.00
$Pyr_{1,2}$	48.70	59.97	62.41	−17.24	17.21
$Mor_{1,e}$	55.80	61.61	68.53	−27.98	11.70
$Mor_{1,2}$	50.30	59.93	65.25	−21.87	15.32
$Mor_{1,4}$	49.50	55.33	66.97	−17.65	15.82
$Mor_{1,8}$	49.10	58.20	67.71	−17.50	16.91
$Pip_{1,e}$	55.65	60.61	68.04	−21.22	16.06
$Pip_{1,g}$	57.00	60.62	67.68	−19.76	15.72
$Aze_{1,4}$	54.50	53.01	64.17	−4.13	23.40
$Aze_{1,e}$	57.44	60.50	68.32	−20.39	17.09

The cation structures are defined in Scheme 1. All quantities are expressed in kcal/mol

[a] Values from Chiappe et. al [10] except from in vacuo value extrapolated reported by Reichardt [34, 35]

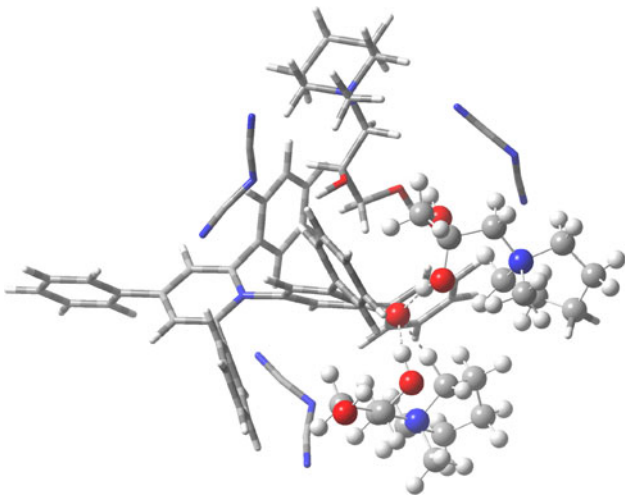

Fig. 2 Coordination of the Pip_{1e} cations and dicyanamide anions with Reichardt's dye. The use of two different representations is for visual purposes only

between a first cation closer to the dye and the second one. The behavior of pyrrolidinium and morpholiniun cations is very similar, practically independent of sidechain length and ring size. The distance and the coordination of the second cation is practically the same. There are small differences for the first cation, but these structures are very similar. It is noteworthy that the oxygen atom on the morpholinium cation is far from the dye. In the case of N-methyl-N-butylazepanium cation, $Aze_{1,4}$, the larger dimension of the ring increases the distance between oxygen dye and IL cation weakening the interaction. These results are consistent with those obtained with MD for the 1-butyl-3-methylimidazolium (BMIM) hexafluorophosphate [9]: there are two well-localized cations about the ET(30) oxygen differing only by orientation. The cations here considered have a different shape and some are functionalized. Furthermore, the methodology used is static and not dynamic. But the coordination number of the ET(30) oxygen is still two.

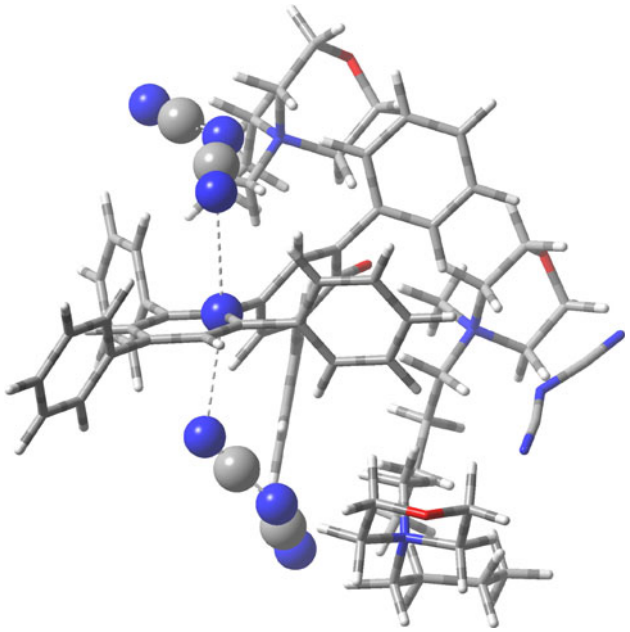

Fig. 3 Coordination of A1 and A2 with ET(30) in the presence of $Mor_{1,4}$ cations. The use of two different representations is for visual purposes only

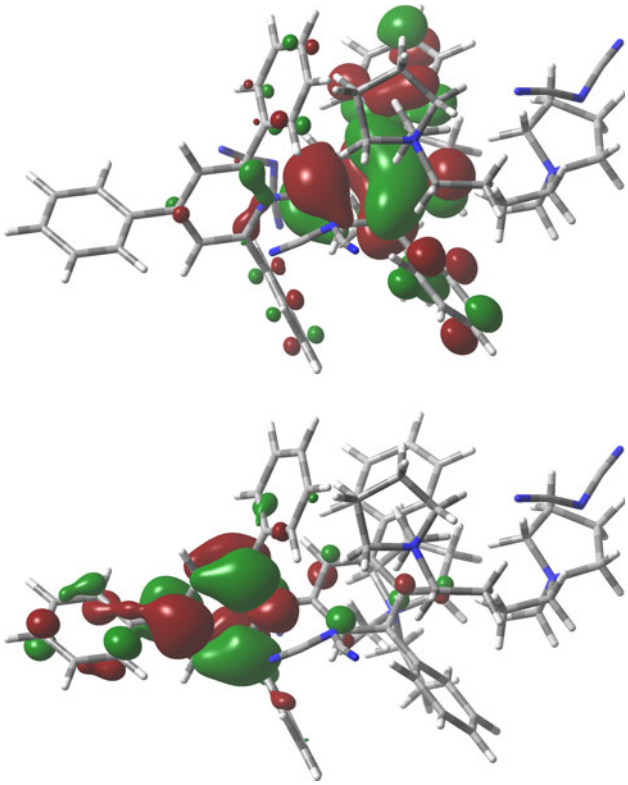

Fig. 4 HOMO (*top*) and LUMO (*bottom*) orbitals for Reichardt's dyes with $Pyr_{1,2}$ dicyanamide first shell of solvation

The anion coordination is very similar in all examined situations. A pictorial example for N-methyl-N-ethylmorpholinium cation, $Mor_{1,2}$, is reported in Fig. 3. The dicyanamide ion is coordinated to the positive nitrogen center of the dye with one of its terminal nitrile nitrogens. This spatial arrangement leaves to the anion two degrees of freedom: it is able to rotate and vary its inclination (see Fig. 3). These two degrees of freedom are, however, partially limited by the surrounding phenyl groups. The anion exploits this feature to pair with the nearest cation that is one of those coordinated at the oxygen center. Consequently, there is an interaction between the species coordinated to the positive and negative sites. We can have a hint of this looking to the difference between the N-A1 and N-A2 distances in relation to the cations coordination patterns. When the two cations are similarly coordinated, as in the case of hydroxyl functionalized cations, N-A1 and N-A2 are very similar. The distances N-A1 and N-A2 increase as the size of the cation ring increases. The coordinating cations are subjected to two electrostatic forces: the ion pairing that reduces the cation–anion distance and the interaction with the dye oxygen that, for sterical reasons, tends to take away the cation from the anion. A small ring has more possibilities to rotate and move than a larger one. Thus, larger cations like $Aze_{1,4}$ are less able to optimize both the interactions. The PF6 anion studied by Kobrak et al. [9] is a spherical top and it is not possible for a direct comparison of the results as in the cation case.

We perform calculation of the ET(30) solvatochromic parameters with CIS/PM6 and ZINDO methods at the PM6 optimized geometries. We discuss the result separately and compare later. These results are reported in Table 2 and, in graphical form in Fig. 5.

Values of the ET(30) parameter calculated at the CIS/PM6 level are largely overestimated with respect the experimental one. There are several motivations to rationalize this behavior, apart the level of calculation. First, we neglect completely the bulk effect. The model system here considered is a small but, in our intention, balanced network of a zwitterion interacting with six ions. These six ions in a real system are influenced by the bulk: other ions can move away or rotate the ions of the first solvation shell. Dynamics phenomena as sidechain conformational motions, ion exchange between first shell and the bulk are totally disregarded. However, some features can be observed. Experimental and calculated values of ET(30) for ILs with the OH moiety lie in a range of 1.3 kcal/mol regardless to size or the presence of heteroatoms on the ring. In the case of $Pyr_{1,2}$, experimental and calculated values of ET(30) are both the lower ones. The low experimental value for $Aze_{1,4}$ is in agreement with the low calculated value. This reduction is probably due to sterical hindering. The series of $Mor_{1,n}$ is different: ET(30)

Scheme 1 Structures of Reichardt's dye, dicyanamide and of cations considered in this paper

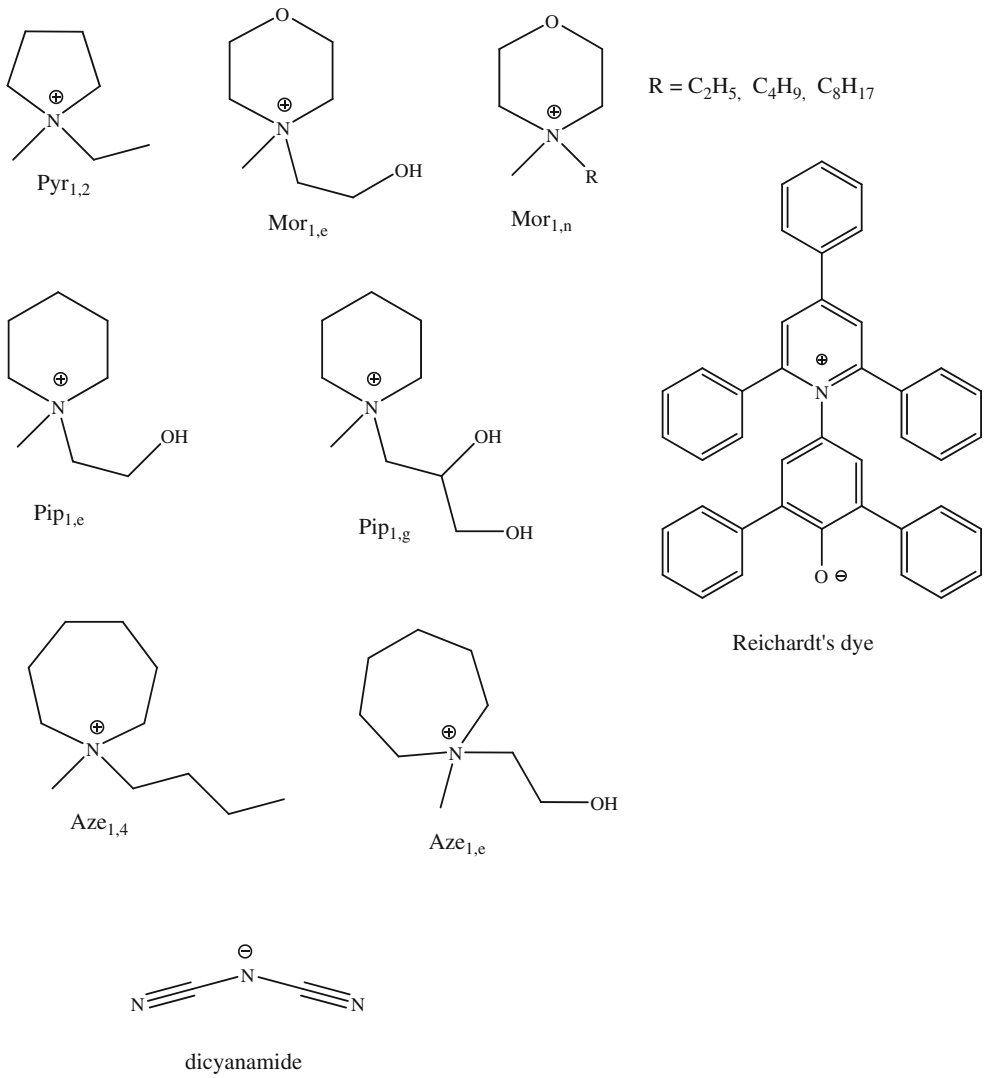

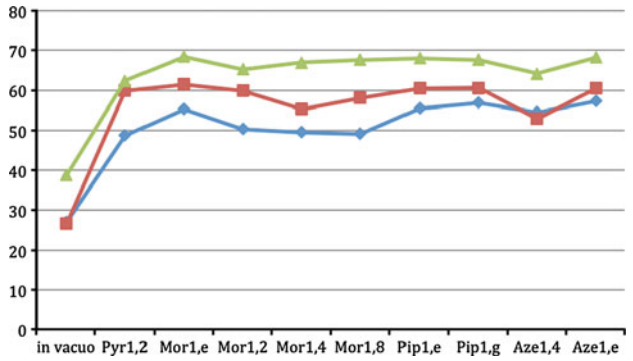

Fig. 5 Graphical representation of ET(30), in Kcal/mol, values obtained by experiment (*blue*/*diamonds*), CIS/PM6 (*green*/*triangles*) and ZINDO (*red*/*squares*)

experimental values decrease when the length of the side-chain increases, but the trend of calculated ones is opposite. Probably, in this case, dynamical and conformational factors cannot be disregarded.

ZINDO results are less overestimated and, in some cases, in good agreement with the experimental results. The value in vacuo is very similar to extrapolated value [34, 35], and thus, we can suppose that the not solvated system is better described by ZINDO than CIS/PM6. The value of $Mor_{1,4}$, obtained with ZINDO, is very different from the $Mor_{1,2}$ and $Mor_{1,8}$ in disagreement with the other two series of data. We have no explanation for this feature. In general, functionalized cations have a ZINDO calculated values that differ by 5 kcal/mol or less where non-functionalized ones differ of about 10 kcal/mol. An exception is $Aze_{1,4}$ value that lies in non-functionalized range. Kobrak [9] stated that in ILs, only the first and second shells are polarized by the Reichardt's dye. A possible interpretation is that in the case of functionalized or sterical hindering cations, the contribution of the second shell is less important, and our small supermolecular model is more similar to the real system. In general, CIS/PM6 values have a better trend but are less accurate than the ZINDO ones.

However, looking at Fig. 5, the presence of a well-defined trend (with the exception, again, of $Aze_{1,4}$) is evident. We decided to avoid a statistical analysis of ET(30) data due to the limited number of values and the heterogeneity of the ILs under investigation.

Table 2 contains also the differences of HOMO and LUMO values with respect the isolated dye. In Fig. 4, a graphical representation of these orbitals is reported. They are very similar to those reported by Caricato et al. [12]; HOMO/LUMO orbitals are stabilized/destabilized by the nearby positive/negative charges of cations/anions, as expected. Since the anion is always the same, the HOMO values are more differentiated than the LUMO ones. The stabilization of functionalized cations is larger, as expected, than the not functionalized ones. The anomaly represented by$Aze_{1,4}$ is reflected also in the orbital energies that show a consistent drift.

4 Conclusions

Solvation of Reichardt's dye in ILs is very different than in molecular solvents. The dimension of the ions, the fact that we added a 1:1 mixture of two very different chemical species, changes completely the scenario. The two extremes of the zwitterion *de facto* interact with different species, the anion and the cation. The balancing between sterical and electrostatic factors seems to be the key factor of ionic liquid–Reichardt's dye interaction. The presence of at least one hydroxyl group on the cation sidechain can overwield these factors. Given these considerations, ET(30) or similar solvatochromic parameters are useful to obtain information about the solvation ability of ILs. However, the agreement of the values here found for ILs with the experimental ones is at a qualitative level only, far from the today standards of computational spectroscopy. This is due to the low level of calculation and to the reduced size of the model system here used.

However, this rough scheme gives some information about the organization of the ionic liquid about the Reichardt's dye. This organization is very different from those of molecular solvents, and thus, a direct comparison can be misleading.

We plan to further extend both experimental and theoretical investigations to reach a better knowledge of the phenomena. Furthermore, a protocol to obtain reliable computational results for excited states of ET(30) needs to be established.

References

1. Wasserscheid P, Welton T (eds) (2007) Ionic liquids in synthesis. Wiley-VCH Weinheim, Germany
2. Chiappe C, Malvaldi M, Pomelli CS (2009) Pure Appl Chem 81(4):767–776
3. Carmichael AJ, Seddon KR (2000) J Phys Org Chem 13:591
4. Aki SNVK, Brennecke JF, Samanta A (2001) Chem Commun 413
5. Reichard C (2004) Pure Appl Chem 76:1903
6. Reichard C (2005) Green Chem 7:339
7. Crowhurst L, Mawdsley PR, Parez-Arlandis JM, Salter PA, Welton T (2001) Phys Chem Chem Phys 3:5192
8. Lee JM, Ruckes S, Prausnitz JM (2008) J Phys Chem B 112:1473
9. Znamenskiy V, Kobrak MN (2004) J Phys Chem B 108: 1072–1079
10. Chiappe C, Pomelli CS, Rajamani S (2011) J Phys Chem B 115(31):9653–9661
11. Dimroth K, Reichardt C, Siepmann T, Bohlmann F (1963) Liebigs Ann Chem 727:93
12. Kamlet MJ, Abboud JML, Taft RW (1981) Progr Phys Org Chem 13:485–630
13. Chiappe C, Malvaldi M, Pomelli CS (2010) J Chem Theory Comp 6:179–183
14. Caricato M, Mennucci B, Tomasi J (2006) Mol Phys 104: 875–887
15. Dewar MJS, Zoebisch EG, Healy EF (1985) J Am Chem Soc 107: 3902
16. Zerne MC (1991) Rev Comp Chem 2:313–366
17. Stewart JJP (2007) J Mol Model 13:1173–1213
18. Stewart JJP (2009) J Mol Model 15:765–805
19. Stewart JJP (2008) J Mol Model 14:499–535
20. Stewart JPP (1989) J Comp Chem 10:209–220
21. Frauenheim T, Seifert G, Elstner M, Hajnal Z, Jungnickel G, Porezag D, Suhai S, Scholz R (2000) Phys Stat Sol B 217:41–62
22. Aradi B, Hourahine B, Frauenheim Th (2007) J Phys Chem B 111(5678):2007
23. Frisch MJ, Trucks GW, Schlegel HB, Scuseria GE, Robb MA, Cheeseman JR, Scalmani G, Barone V, Mennucci B, Petersson GA, Nakatsuji H, Caricato M, Li X, Hratchian HP, Izmaylov AF, Bloino J, Zheng G, Sonnenberg JL, Hada M, Ehara M, Toyota K, Fukuda R, Hasegawa J, Ishida M, Nakajima T, Honda Y, Kitao O, Nakai H, Vreven T, Montgomery Jr. JA, Peralta JE, Ogliaro F, Bearpark M, Heyd JJ, Brothers E, Kudin KN, Staroverov VN, Kobayashi R, Normand J, Raghavachari K, Rendell A, Burant JC, Iyengar SS, Tomasi J, Cossi M, Rega N, Millam NJ, Klene M, Knox JE, Cross JB, Bakken V, Adamo C, Jaramillo J, Gomperts R, Stratmann RE, Yazyev O, Austin AJ, Cammi R, Pomelli C, Ochterski JW, Martin RL, Morokuma K, Zakrzewski VG, Voth GA, Salvador P, Dannenberg JJ, Dapprich S, Daniels AD, Farkas Ö, Foresman JB, Ortiz JV, Cioslowski J, Fox DJ (2009) Gaussian 09, revision A.1. Gaussian Inc., Wallingford
24. Foresman JB, Head-Gordon M, Pople JA, Frisch MJ (1992) J Phys Chem 96:135–149
25. Mennucci B, Cances E (1997) Tomasi. J Phys Chem B 101: 10506–10517
26. Mizoshiri M, Nagao T, Mizoguchi Y, Yao M (2010) J Chem Phys 132(164510):1–7
27. Huang MM, Jiang Y, Sasisanker P, Driver GW (2011) J Chem Eng Data 56:1494–1499
28. Bini R, Chiappe C, Pomelli CS, Parisi B (2009) J Org Chem 74:8522–8530
29. Bini R, Chiappe C, Mestre VL, Pomelli CS, Welton T (2009) Theor Chem Acc 123:347–352
30. Pomelli CS, Chiappe C, Vidis A, Laurenczy G, Dyson PJ (2007) J Phys Chem B 111:13014–13019
31. Hunt P, Kirchner B, Welton T (2010) Chem Eur J 12:6762–6775
32. Peng C, Ayala PY, Schlegel HB, Frisch MJ (1996) J Comp Chem 17:49–56
33. Császár P, Pulay P (1984) J Mol Struct 114:31–34
34. Reichardt C (2004) Solvent effects in organic chemistry, 3rd updated and enlarged edition. Wiley-VCH Weinheim, Germany
35. Lindner B (1992) J Phys Chem 96:10708–10712